Inorganic Chemistry

pubs.acs.org/IC

Featured Article

Next Generation Cuprous Phenanthroline MLCT Photosensitizer Featuring Cyclohexyl Substituents

Michael C. Rosko, Kaylee A. Wells, Cory E. Hauke, and Felix N. Castellano*

Cite This: https://doi.org/10.1021/acs.inorgchem.1c01242

Read Online

ABSTRACT: A new long-lived, visible-light-absorbing homoleptic Cu(I) metal-to-ligand charge transfer (MLCT) photosensitizer, $[Cu(dchtmp)_2]PF_6$ (dchtmp = 2,9-dicyclohexyl-3,4,7,8-tetramethyl-1,10-phenanthroline), has been synthesized, structurally characterized, and evaluated in terms of its molecular photophysics, electrochemistry, and electronic structure. Static and time-resolved transient absorption (TA) and photoluminescence (PL) spectroscopy measured on the title compound in CH_2Cl_2 (τ = 2.6 μs, Φ_{PL} = 5.5%), CH_3CN (τ = 1.5 μs, Φ_{PL} = 2.6%), and THF (τ = 2.0 μs, Φ_{PL} = 3.7%) yielded impressive photophysical metrics even when dissolved in Lewis basic solvents. The combined static spectroscopic data along with ultrafast TA experiments revealed that the pseudo-Jahn−Teller distortion and intersystem crossing dynamics in the MLCT excited state displayed characteristics of being sterically arrested throughout its evolution. Electrochemical and static PL data illustrate that $[Cu(dchtmp)_2]PF_6$ is a potent photoreductant (−1.77 V vs $Fc^{+/0}$ in CH_3CN) equal to or greater than all previously investigated homoleptic Cu(I) diimine complexes. Although we successfully prepared the cyclopentyl analog dcptmp (2,9-dicyclopentyl-3,4,7,8-tetramethyl-1,10-phenanthroline) using the same C−C radical coupling photochemistry as dchtmp, the corresponding Cu(I) complex could not be isolated due to the steric hindrance presented at the metal center. Ultimately, the successful preparation of $[Cu(dchtmp)_2]^+$ represents a major step forward for the design and discovery of novel earth-abundant photosensitizers made possible through a newly conceived ligand synthetic strategy.

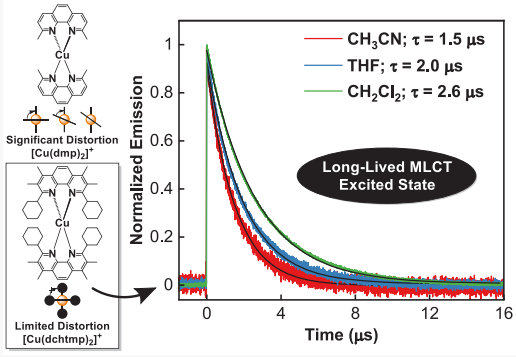

■ INTRODUCTION

Visible-light activated chemistry using heavy metal photosensitizers has realized numerous photoredox applications that present numerous challenges in large-scale photocatalytic applications.[1−4] One key aspect toward advancing this technology relies on the development of new charge transfer photosensitizers, both metal-to-ligand and ligand-to-metal charge transfer, MLCT and LMCT, respectively, featuring first-row transition metals. Numerous molecules based on first-row transition metals traditionally suffer from significant excited state quenching due to energetically-accessible ligand field states.[5−9] Copper(I) *bis*(diimine) chromophores featuring $3d^{10}$ electron configurations completely eliminate ligand-field state influence in excited state decay. However, as a consequence of the MLCT nature of their excited states, Cu(I) diimine-based photosensitizers suffer from deactivating pseudo-Jahn−Teller (PJT) distortions resulting from transient production of the Cu(II) $3d^9$ electron configuration.

The effects of the PJT distortions on the photophysical behavior of Cu(I) *bis*(phenanthrolines) have been extensively studied since the 1970s.[10−31] Once excited into the singlet metal-to-ligand charge transfer (^{1}MLCT) excited state, which effectively oxidizes Cu(I) to Cu(II), which is a d^9 configuration, the diimine ligands engage in a flattening distortion due to the unequal occupation of degenerate d orbitals.[32] This geometric relaxation wastes the potential energy stored in the excited state. Upon flattening, the metal center becomes susceptible to nucleophilic attack from counterions and/or Lewis basic solvents, with one notable exception,[33] ultimately leading to short-lived excited states.[34−37] Figure 1a presents a simplified energy level diagram depicting the relative time constants for these aforementioned processes.[27,38−41] Theoretical calculations from Nozaki and co-workers[42] originally deduced that the time constant of intersystem crossing for Cu(I) *bis*(diimines) with excited state distortion should lengthen while the radiative rate constant decreases, as was later experimentally demonstrated by Tahara and co-workers.[43]

The PJT distortions characteristic in the MLCT excited states of Cu(I) *bis*(diimines) can be markedly reduced through structural engineering by incorporating bulky 2,9-alkyl substituents on the phenanthroline ligands, thereby extending

Received: April 22, 2021

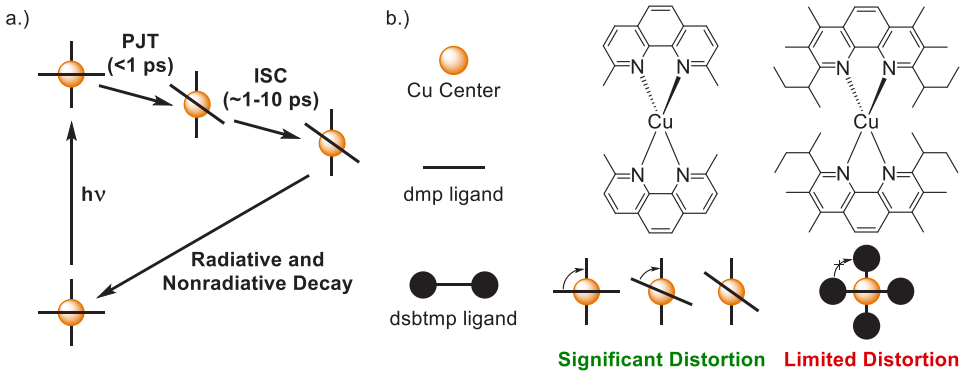

Figure 1. (a) Qualitative energy level diagram of the photophysical processes in Cu(I) *bis*(diimines) including the PJT distortion and intersystem crossing (ISC) time scales resulting in the molecule returning to the ground state either through radiative or nonradiative decay. (b) Illustration of the extent of the PJT distortion in $[Cu(dmp)_2]^+$ (left) and $[Cu(dsbtmp)_2]^+$ (right).

the excited state lifetimes.[19,26,31,34,44−46] McMillin and co-workers more recently discovered that 3,8-methylation of phenanthroline further extends the Cu(I) MLCT excited state lifetime through cooperative steric enhancement of the 2,9-substituents, resulting in less excited state distortion and more complete shielding of the copper center from the surrounding environment.[47] Our laboratory has previously leveraged branched alkyl substituents paired with McMillin's 3,8-methylation strategy resulting in microsecond Cu(I) MLCT lifetimes and high quantum yield photoluminescence at RT.[48−50] A depiction of how the PJT distortion is restricted using our structural design is presented in Figure 1b, which directly compares a traditional Cu(I) MLCT photosensitizer $[Cu(dmp)_2]PF_6$ (dmp = 2,9-dimethyl-1,10-phenanthroline) to the one conceived in our laboratory, $[Cu(dsbtmp)_2]PF_6$ (dsbtmp = 2,9-di(*sec*-butyl)-3,4,7,8-tetramethyl-1,10-phenanthroline).

The broadly accepted synthetic methodology for installing alkyl substituents on the 2- and 9-positions of 1,10-phenanthroline uses traditional alkyl/aryllithium reagents as originally pioneered by Sauvage et al.[19,21,25,45,47−51] Limitations to this two-electron route become obviated as many desirable synthons are not readily available or easily prepared. A facile photocatalytic radical pathway was recently developed by Glorius and co-workers to synthesize numerous heterocycles, including 2,9-di(cyclohexyl)-3,4,7,8-tetramethyl-1,10-phenanthroline (dchtmp).[52] In our hands, this diimine ligand was synthetically inaccessible using the Sauvage strategy, and the Glorius approach represents a pathway to a new class of Cu(I) *bis*(diimine) photosensitizers featuring 2,9-cycloalkyl substituents (Chart 1). $[Cu(dchtmp)_2]PF_6$ is the first member of this class. We successfully synthesized 2,9-di(cyclopentyl)-3,4,7,8-tetramethyl-1,10-phenanthroline (dcptmp) through the same photochemical radical coupling chemistry. However, the corresponding Cu(I) complex $[Cu(dcptmp)_2]PF_6$ did not form as a stable product, a fact that provides interesting insights into the limits of steric influence that can be exerted at the 2,9 positions of phenanthroline. $[Cu(dchtmp)_2]PF_6$ possesses an excited state lifetime (τ = 2.6 μs), photoluminescence quantum yield (Φ = 5.5%), and redox properties similar to those of the champion $[Cu(dsbtmp)_2]PF_6$,[48] thus demonstrating that the more compact cycloalkyl group provides similar inhibition of the PJT distortion, imparting similarly beneficial photophysical properties with respect to using branched alkyl groups without introducing chiral centers into the ligand framework.

Chart 1. Molecular Structures of dchtmp, dcptmp, $[Cu(dchtmp)_2]^+$, and the Hypothetical $[Cu(dchtmp)_2]^+$

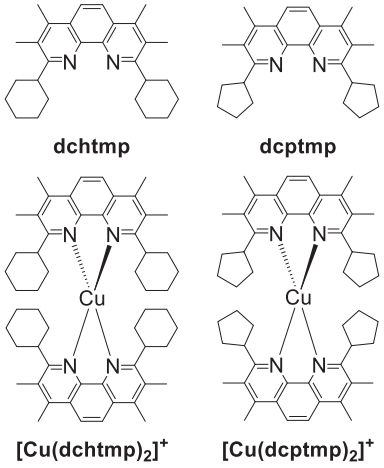

EXPERIMENTAL SECTION

General Procedures. All reagents were purchased from Sigma-Aldrich, Alfa Aesar, or TCI and were used without further purification. Spectroscopy samples were prepared using spectrophotometric grade solvents. The $[Ir(ppy)_2(dtbbpy)]PF_6$ photocatalyst was synthesized using an established literature procedure.[53] All spectrophotometric samples were deaerated using the freeze−pump−thaw technique, prepared in an inert N_2-filled gas glovebox, or purged with N_2 gas. ^{1}H and ^{13}C NMR measurements were executed on a Bruker Avance 400 or 700 MHz spectrometer. All NMR spectra were processed using the MNova 10.0 software package. Mass spectrometry was performed by the Michigan State University Mass Spectrometry Core, East Lansing, MI. Elemental analysis was performed by Atlantic Microlab, Inc., Norcross, GA. All NMR and mass spectra are provided in the Supporting Information (Figures S1−S10).

Electronic absorption spectra were measured using a Cary 60 UV/vis spectrophotometer or a Shimadzu UV-3600 spectrometer. Static photoluminescence (PL) spectra were collected with a FLS980 fluorometer (Edinburgh Instruments) equipped with a 450 W Xe arc lamp and a R2658P PMT detector (Hamamatsu); measurements were corrected for detector response. Quantum yield measurements were recorded using a FS5 fluorometer (Edinburgh Instruments) equipped with an integrating light sphere (absolute). All spectral PL and absorption measurements were performed using optically dilute samples (OD = 0.1−0.2) at the excitation wavelength (450 nm).

Syntheses. *2,9-Dicyclopentyl-3,4,7,8-tetramethyl-1,10-phenanthroline (dcptmp).* The preparation was adapted from Glorius and co-workers.[52] 3,4,7,8-Tetramethylphenanthroline (71 mg, 0.300

https://doi.org/10.1021/acs.inorgchem.1c01242
Inorg. Chem. XXXX, XXX, XXX−XXX

mmol, 1.0 equiv), 1-cyclopentyl-2,4,6-triphenylpyridinium tetrafluoroborate (417 mg, 0.900 mmol, 3.0 equiv), $[Ir(ppy)_2(dtbbpy)]PF_6$ (6.9 mg, 2.5 mol %), and *N,N*-dimethylacetamide (1.5 mL) were added to a 10 mL microwave reaction vessel. The solution was sparged with N_2 gas for 20 min, then irradiated with a 456 nm PR160L Kessil lamp held 2−4 cm from the reaction vessel with continuous sparging maintained for 48 h (Figure S11). After irradiation, triethylamine (0.3 mL) was added to the vessel and vigorously stirred for 20 min. The resulting solution was diluted with ethyl acetate (30 mL) and washed with deionized water (1 × 25 mL) and brine (3 × 25 mL). The organic layer was dried with $MgSO_4$ and vacuum filtered to remove the solid. Solvent was removed and the crude product was dried onto silica via rotary evaporation and purified on silica using a CombiFlash NextGen 300+ automated flash chromatography system from Teledyne ISCO (eluent 3:1 petroleum ether/ethyl acetate; R_f = 0.6) and was isolated as a white solid (28.0 mg, 0.075 mmol, 24% yield). ^{1}H NMR (400 MHz; $CDCl_3$; Figure S5): δ 7.91 (s, 2H); 3.72−3.63 (m; 2H); 2.66 (s, 6H); 2.50 (s, 6H); 2.39−2.25 (m, 4H); 2.21−2.07 (m, 4H); 2.06−1.92 (m, 4H); 1.82−1.68 (m, 4H). ^{13}C NMR (100 MHz; $CDCl_3$; Figure S6): δ 162.27; 142.36; 139.42; 127.29; 124.54; 120.02; 44.15; 30.80; 25.20; 14.47; 13.87.

[Cu(dchtmp)$_2$]PF$_6$. In a round-bottom flask, dchtmp (82.1 mg, 0.21 mmol, 2.1 equiv) was dissolved in dichloromethane (10 mL) and sparged with N_2 gas. The solution was cannula transferred into a Schlenk flask containing tetrakis(acetonitrile)copper(I)-hexafluorophosphate[54] (36.9 mg, 0.099 mmol, 1.0 equiv) under a nitrogen atmosphere, the resulting solution changing immediately to dark orange. Diethyl ether was added to the solution to precipitate an orange solid, and the solution was placed in a freezer overnight to induce further precipitation. The product (51.4 mg, 0.051 mmol, 51% yield) was collected via vacuum filtration, washed with diethyl ether, and dried in a vacuum oven. ^{1}H NMR (400 MHz; $CDCl_3$; Figure S7): δ 8.21 (s, 4H); 3.42 (t, 4H); 2.79 (s, 12H); 2.60 (s, 12H); 2.79 (s, 12H); 1.81−1.70 (m, 8H); 1.39−1.34 (m, 8H); 1.25−1.19 (m, 8H); 1.13−1.07 (m, 4H); 0.81 (broad s, 4H); −0.25 (broad s, 4H). ^{13}C NMR (175 MHz; $CDCl_3$; Figure S8): δ 162.13; 145.40; 141.78; 131.79; 126.82; 122.46; 429.72; 26.31; 25.47; 17.18; 15.61. MS-TOF (CH_3OH) *m/z*: 863.5029 $[M-PF_6]^+$. Calcd. ($C_{56}H_{72}CuN_4$): 863.5053 (Figure S10). Elemental analysis calculated for $C_{56}H_{72}CuN_4F_6P{\cdot}0.1H_2O{\cdot}0.2CH_3Cl$: C, 65.19; H; 7.05; N, 5.41. Experimental: C, 64.96; H; 6.99; N, 5.42.

Nanosecond Transient Absorption and Time-Resolved Photoluminescence Spectroscopy. Nanosecond transient absorption (TA) and PL measurements were acquired using a LP920 laser flash photolysis system from Edinburgh Instruments. A Vibrant 355 Nd:YAG/OPO system (OPOTEK) was used as the pulsed laser excitation source with a pulse energy of 1.6 mJ/pulse at 450 nm. An iStar ICCD camera (Andor Technology) was used to collect transient absorption spectra, and a R2658P PMT detector (Hamamatsu) was used to collect kinetic absorption and kinetic emission data, controlled by the LP920 software (Edinburgh Instruments). Samples were degassed using three freeze−pump−thaw cycles in 1 cm path length quartz optical cells. Samples were prepared with optical densities between 0.3 and 0.5 at the excitation wavelength (450 nm). Variable temperature emission decays were obtained with a CoolSpek UV Cryostat (Unisoku Scientific Instruments). The same was measured in a 1 cm quartz cuvette with an optical density of 0.15 using THF as the solvent. Measurements were taken between −100 and 60 °C after 10 min at each temperature to allow the solution to equilibrate. Kinetic traces were fit with single exponential functions using OriginPro 2020b software.

Photosensitization. Solutions containing 0.077 mM $[Cu(dchtmp)_2]PF_6$ were prepared for photosensitization with 9,10-diphenylanthracene (DPA) as the acceptor. Static PL spectra were collected with a FLS980 fluorometer (Edinburgh Instruments) equipped with a 450 W Xe arc lamp under 488 nm excitation. A Vibrant 355 Nd:YAG/OPO system (OPOTEK) was used as the pulsed laser excitation source with a pulse energy of 1.8 mJ/pulse at 488 nm. A R2658P PMT detector (Hamamatsu) was used to collect kinetic emission data, controlled by the LP920 software (Edinburgh Instruments). Kinetic traces were fit with single exponential functions, and the dynamic Stern−Volmer plot was fit with a linear regression curve using OriginPro 2020b.

Ultrafast Transient Absorption Spectroscopy. Ultrafast transient absorption measurements were performed at the NCSU Imaging and Kinetics Spectroscopy Laboratory using a Helios transient absorption spectrometer from Ultrafast Systems. A 1 kHz Ti:sapphire Coherent Libra regenerative amplifier (4 mJ/pulse, 105 fs (fwhm) at 800 nm) was split into the pump and probe beams. The probe beam was delayed in a 6 ns optical delay stage while the pump beam was directed into a parametric amplifier (Coherent OPerA Solo) to generate 425 nm light for excitation. Transient absorption measurements were performed between 350 and 750 nm using a CaF_2 crystal to generate the white-light continuum. The pump beam (∼700 μm) was overlapped with the probe beam through a 2 mm cuvette while being stirred. Optical densities for samples were maintained between 0.2 and 0.3 at the 425 nm excitation wavelength. The ground state absorption spectra were taken before and after the TA experiments, ensuring that there was no photodegradation. Transient difference spectra and single wavelength kinetics were processed using OriginPro 2020b software.

Electrochemistry. Electrochemical measurements were performed in an inert glovebox atmosphere (MBraun) using 0.1 M TBAH in acetonitrile as the supporting electrolyte; CH_3CN used in experiments was dried and degassed in an MBraun SPS solvent purification system. Cyclic voltammetry (CV) and differential pulse voltammetry (DPV) experiments were performed using a three-electrode arrangement featuring a platinum disk working electrode (1.6 mm), a platinum wire counter electrode, and an $Ag/AgNO_3$ reference electrode. A ferrocenium/ferrocene ($Fc^{+/0}$) internal standard was used as a reference in all electrochemical potential measurements. All voltammograms were recorded with a Bioanalytical Systems (BASi) Epsilon potentiostat and processed with OriginPro 2020b software.

Computational Methods. Density functional theory (DFT) and time-dependent density functional theory (TD-DFT) calculations were performed using the Gaussian 16 software package[55] in concert with the computational resources available at the North Carolina State University High Performance Computing Center. Ground state and triplet state structural optimizations were calculated at the (U)B3LYP+D3//6-311G* level of theory for hydrogen, carbon, and nitrogen atoms.[56−59] An SDD basis set was applied to the copper atom accompanied by an effective core potential.[60] The polarizability continuum model (PCM) was applied to all molecules using dichloromethane as the solvent environment.[61] Frequency calculations were performed to ensure that the geometries were at an energy minimum, and no imaginary frequencies were found. Dihedral angles were measured from the interior carbons of both ligands. All optimized structures were visualized using GaussView 6.0.[62]

■ RESULTS AND DISCUSSION

Electronic Structure Calculations. DFT-optimized ground (S_0) and lowest triplet excited state (T_1) structures of the stable Cu(I) complexes $[Cu(dmp)_2]^+$, $[Cu(dsbtmp)_2]^+$, and $[Cu(dchtmp)_2]^+$ as well as the hypothetical $[Cu(hmp)_2]^+$ (hmp = 2,3,4,7,8,9-hexamethyl-1,10-phenanthroline) are presented in Chart 2. In the ground state, the dihedral angle between the two diimine ligands in each molecule was calculated as 89.3°, 87.1°, 87.1°, and 87.5° for $[Cu(dmp)_2]^+$, $[Cu(hmp)_2]^+$, $[Cu(dsbtmp)_2]^+$, and $[Cu(dchtmp)_2]^+$, respectively. The ground state dihedral angles appear to have minimal differences with respect to one another, with $[Cu(dsbtmp)_2]^+$ and $[Cu(dchtmp)_2]^+$ having nearly equal but slightly offset dihedral angles likely due to the differences in the steric bulk in their respective 2,9-positions. The T_1 dihedral angles were calculated to be 60.6°, 59.4°, 77.0°, and 77.0° for $[Cu(dmp)_2]^+$, $[Cu(hmp)_2]^+$, $[Cu(dsbtmp)_2]^+$, and

https://doi.org/10.1021/acs.inorgchem.1c01242
Inorg. Chem. XXXX, XXX, XXX−XXX

Chart 2. DFT-Optimized Ground State and Lowest Energy Triplet Structures of $[Cu(dmp)_2]^+$, $[Cu(hmp)_2]^+$, $[Cu(dsbtmp)_2]^+$, and $[Cu(dchtmp)_2]^+$ Optimized at the (U)B3LYP+D3//6-311G*/SDD Level of Theory in a Dichloromethane Solvent Continuum

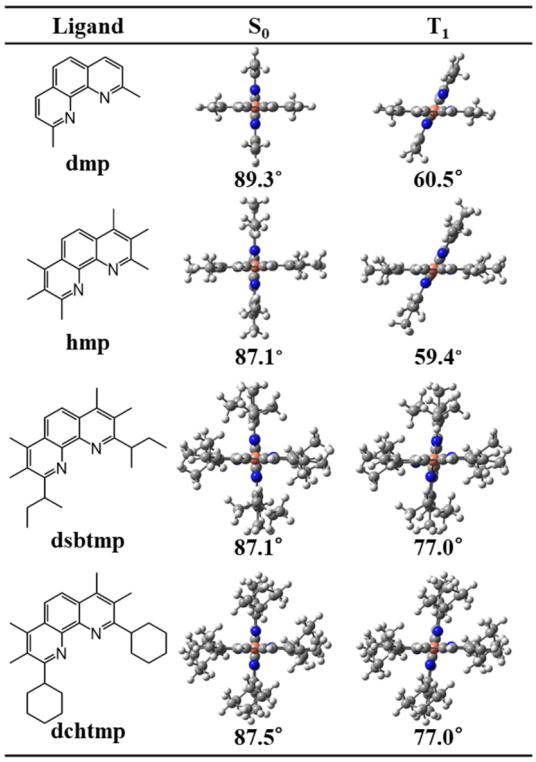

$[Cu(dchtmp)_2]^+$, respectively. The dihedral angles calculated for $[Cu(dsbtmp)_2]^+$ and $[Cu(dchtmp)_2]^+$ are nearly identical yet remain significantly larger than that of $[Cu(dmp)_2]^+$, which lacks the 3,8-dimethyl substituents, and $[Cu(hmp)_2]^+$ featuring 2,9-dimethyl substituents. The singlet−triplet dihedral angle difference suggests the extent of the PJT distortion in the lowest energy triplet excited state. The largest differences were calculated in $[Cu(dmp)_2]^+$ (28.7°) and $[Cu(hmp)_2]^+$ (27.7°). $[Cu(dsbtmp)_2]^+$ and $[Cu(dchtmp)_2]^+$ share similar dihedral angle differences (10.1° and 10.5°), suggesting that the PJT distortion is anticipated to be significantly suppressed in $[Cu(dchtmp)_2]^+$.[63]

Syntheses. The dchtmp ligand was prepared as described by Glorious and co-workers through deaminative visible-light mediated generation of alkyl radicals from the corresponding Katritzky salt.[52] The same reaction pathway (Scheme 1) also proved successful in forming the dcptmp ligand. In the latter case, the Katritzky salt precursor was readily prepared from commercially available 2,4,6-triphenylpyrylium tetrafluoroborate and cyclopentylamine. The isolated product was subsequently reacted with 3,4,7,8-tetramethyl-1,10-phenanthroline and the $[Ir(ppy)_2(dtbbpy)]PF_6$ photocatalyst under intense blue excitation (λ_{ex} = 456 nm) over the course of 2 days under a N_2 atmosphere, producing dcptmp. This reaction represents a useful alternative to those incorporating alkyllithium reagents, as originally pioneered by Sauvage and co-workers,[51] especially in cases where the corresponding cycloalkyllithium is not easily formed. The dchtmp and dcptmp ligands were isolated in sufficient yield to proceed to the final step to prepare the respective Cu(I) MLCT photosensitizers.

The title complex, $[Cu(dchtmp)_2]PF_6$, was prepared according to previous literature procedures used for related *bis*(diimine) Cu(I) complexes.[64] In contrast to the previously synthesized $[Cu(dsbtmp)_2]PF_6$ chromophore, the newly conceived $[Cu(dchtmp)_2]PF_6$ molecule lacks ligand-based chiral centers and thus avoids the creation of diasteromers.[48] Interestingly, the synthesis of $[Cu(dcptmp)_2]PF_6$ was unsuccessful, despite repeated attempts using a variety of reaction conditions. ^{1}H NMR analysis indicated that the recovered solid from these reactions was the uncoordinated dcptmp ligand. Geometry optimization calculations performed on the hypothetical molecule $[Cu(dcptmp)_2]^+$ were used to help rationalize why it was unable to be isolated. The optimized molecular geometry shows that the 2,9-cyclopentyl moieties adopt a half-chair conformation, disrupting the chelation of the second dcptmp ligand, forcing it out-of-plane, leading to irregular dihedral angles as indicated in Figure 2. Similar behavior has also been previously reported for $[Cu(dtbp)_2]^+$ (dtbp = 2,9-di(*tert*-butyl)-1,10-phenanthroline).[25] The failure of this particular coordination reaction illustrates that the conformation(s) adopted by the cycloalkane substituents appended at the 2,9 positions of phenanthroline are crucial for yielding the desired homoleptic Cu(I) complex.

Electrochemistry. Electrochemical data for $[Cu(dchtmp)_2]PF_6$ are given in Table 1, referenced to the $Fc^{+/0}$ redox couple, along with comparable data previously reported for $[Cu(dsbtmp)_2]PF_6$. $[Cu(dchtmp)_2]PF_6$ was subjected to both cyclic and differential pulse voltammetry (Figures S12 and S13) in order to evaluate the ground-state redox potentials. A reversible one-electron $Cu^{II/I}$ oxidation of $[Cu(dchtmp)_2]PF_6$ was detected at 0.43 V vs $Fc^{+/0}$. Two reversible reduction waves were measured at −2.38 and −2.60

Scheme 1. (i) 2,4,6-Triphenylpyrylium Tetrafluoroborate, EtOH (85°C, 4 h); (ii) 3,4,7,8-Tetramethyl-1,10-phenanthroline, $[Ir(ppy)_2(dtbbpy)](PF_6)$, N,N-Dimethylacetamide (λ_{ex} = 456 nm, 48 h); (iii) $[Cu(CH_3CN)_4]PF_6$, CH_2Cl_2 (rt)

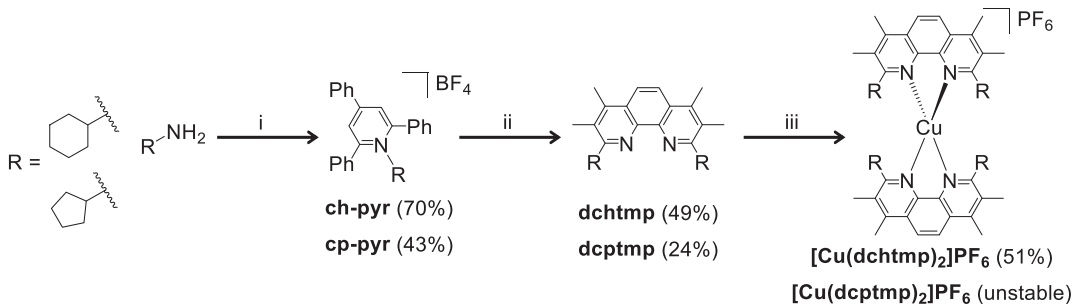

https://doi.org/10.1021/acs.inorgchem.1c01242
Inorg. Chem. XXXX, XXX, XXX−XXX

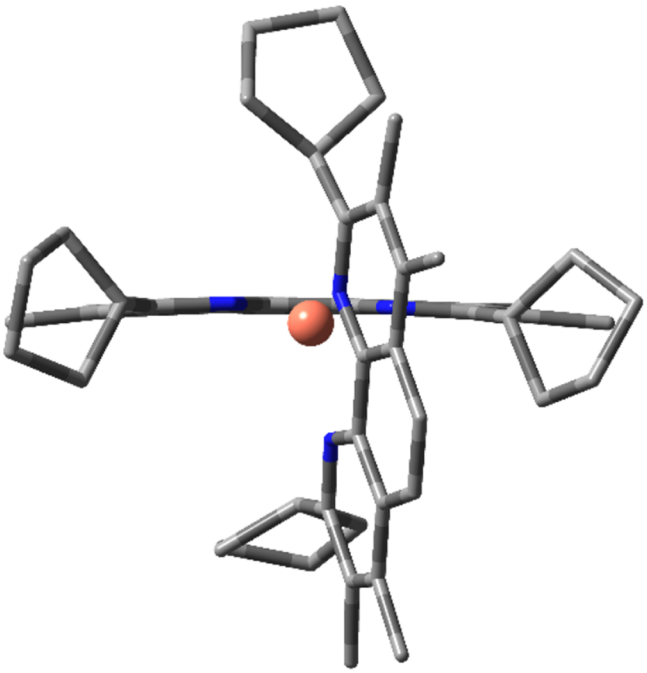

Figure 2. Images of the DFT-optimized ground-state molecular structure of $[Cu(dcptmp)_2]^+$ optimized at the B3LYP/6-311G* level of theory in a dichloromethane solvent continuum. Ligands appear out-of-plane with respect to the Cu(I) center, suggesting instability of the proposed molecule.

Table 1. Electrochemical Data Measured for $[Cu(dsbtmp)_2]PF_6$ and $[Cu(dchtmp)_2]PF_6$ in 0.1 M TBAH in CH_3CN[a]

	E_{ox} (V)	E_{red} (V)	E_{00} (V)[c]	E_{ox}^* (V)[d]	E_{red}^* (V)[d]
$[Cu(dsbtmp)_2]PF_6$[b]	0.428	−2.38 −2.59	2.20	−1.77	−0.18
$[Cu(dchtmp)_2]PF_6$	0.43	−2.38 −2.60	2.20	−1.77	−0.18

[a]Potentials are measured by CV and DPV in CH_3CN solutions with 0.1 M TBAH as the supporting electrolyte vs $Ag/AgNO_3$. Measurements are reported relative to $Fc^{+/0}$ standard. [b]From ref 48. [c]E_{00} estimated by tangent line drawn on blue edge of the PL emission spectrum in CH_3CN (Figures S14 and S15). [d]$E_{ox}^* = E_{ox} - E_{00}$ and $E_{red}^* = E_{red} + E_{00}$.

V, each representing the reduction of the phenanthroline ligands to their respective radical anion species. The E_{00} energy of both species was approximated with a tangent line drawn on the blue edge of the PL emission spectra in CH_3CN, where the x intercept is E_{00} (Figures S14 and S15). The estimated excited state reduction potential of the $Cu^{II/I*}$ couple in $[Cu(dchtmp)_2]PF_6$ is −1.77 V (vs $Fc^{+/0}$), suggesting that this Cu(I) photosensitizer is a potentially potent photoreductant that exceeds the excited state potential of the benchmark MLCT chromophore $[Ru(bpy)_3]^{2+}$ (−1.21 V in CH_3CN vs $Fc^{+/0}$)[65] along with many other earth-abundant MLCT photoreductants.[66] The electrochemical properties reported here echo those of the previously reported $[Cu(dsbtmp)_2]PF_6$ complex.

Static Absorption and PL Measurements. The electronic absorption and PL spectra of $[Cu(dchtmp)_2]PF_6$ measured in CH_2Cl_2 are presented in Figure 3. The two most intense absorption features appear at 280 and 455 nm. The former is assigned to the $\pi-\pi^*$ transitions localized in the diimine ligand,[67] while the latter is assigned to the MLCT transitions (Figure 3a).[68] The spectral profile of the low energy MLCT absorption band provides evidence for the ground state geometry of the complex in solution.[69] Notably, both MLCT and $\pi-\pi^*$ transitions of the title compound mirror those of $[Cu(dsbtmp)_2]PF_6$ both structurally and energetically.[48] If the ground-state geometry of the Cu(I) photosensitizer deviates away from a pseudotetrahedral D_{2d} structure toward a more distorted D_2 symmetry, a red shoulder will become apparent on the MLCT band as the lowest energy charge transfer transition becomes allowed in this geometry.[42] With the presence of only a weak tail on the red edge of the MLCT band, the data suggest $[Cu(dchtmp)_2]PF_6$ tends toward an optimal pseudotetrahedral geometry, much like $[Cu(dsbtmp)_2]PF_6$, rather than exhibiting a more distorted/flattened D_2 geometry."

The PL maximum of $[Cu(dchtmp)_2]PF_6$ in deaerated CH_2Cl_2 is 631 nm (Figure 3b). This PL band is broad and featureless, in accordance with phosphorescence originating from the ^{3}MLCT excited state.[68] The quantum yield and PL lifetime are reported in Table 2, along with those previously reported for $[Cu(dsbtmp)_2]PF_6$. $[Cu(dchtmp)_2]PF_6$ has a 2.6 μs excited state lifetime and a 5.5% quantum yield in deaerated CH_2Cl_2, both quantitatively comparable to the 2.8 μs lifetime and 6.3% quantum yield of $[Cu(dsbtmp)_2]PF_6$.[38] CH_3CN and THF were utilized to evaluate the photophysical characteristics of the title chromophore in more polar, Lewis basic solvents. The PL maxima of $[Cu(dchtmp)_2]PF_6$ in THF and CH_3CN red-shift to 639 and 650 nm, respectively. This is again nearly identical behavior to that previously observed for $[Cu(dsbtmp)_2]PF_6$. Across all solvents, $[Cu(dchtmp)_2]PF_6$ exhibits excited-state lifetimes in the microsecond time regime (Table 2 and Figure S16). The presence of a long-lived excited-state in CH_3CN points to the suppression of exciplex formation with the Lewis basic coordinating solvent, not surprising given the collective data presented above. In comparison to $[Cu(dsbtmp)_2]PF_6$, the radiative and nonradiative rates of decay obtained for $[Cu(dchtmp)_2]PF_6$ in CH_2Cl_2, THF, and CH_3CN are nearly identical (Table 2), indicating strong parallels between their respective nonradiative deactivation pathways. We therefore conclude that the 2,9-cyclohexyl substituents successfully shield the Cu(I) center from the solvent environment in both ground and excited states of $[Cu(dchtmp)_2]^+$.

Dynamic PL quenching of $[Cu(dchtmp)_2]PF_6$ in the presence of 9,10-diphenylanthracene (DPA) measured in CH_2Cl_2 is presented in Figure S17. Selective 488 nm pulsed excitation of $[Cu(dchtmp)_2]PF_6$ as a function of increasing DPA concentration resulted in a linear Stern−Volmer plot (Figure S18) from the resultant lifetime data, eq 1:

$$\frac{\tau_0}{\tau} = 1 + K_{SV}[Q] \quad (1)$$

where K_{SV} is the Stern−Volmer constant and k_q is the bimolecular quenching constant, τ_0 and τ are the PL lifetimes in the absence or presence of DPA, and [Q] is the molar concentration of DPA. The K_{SV} and k_q values were determined to be 735 M^{-1} and 2.82×10^8 M^{-1} s^{-1}, respectively (Figure S18), for the triplet−triplet energy transfer process occurring between the energized Cu(I) photosensitizers and ground state DPA molecules.

https://doi.org/10.1021/acs.inorgchem.1c01242
Inorg. Chem. XXXX, XXX, XXX−XXX

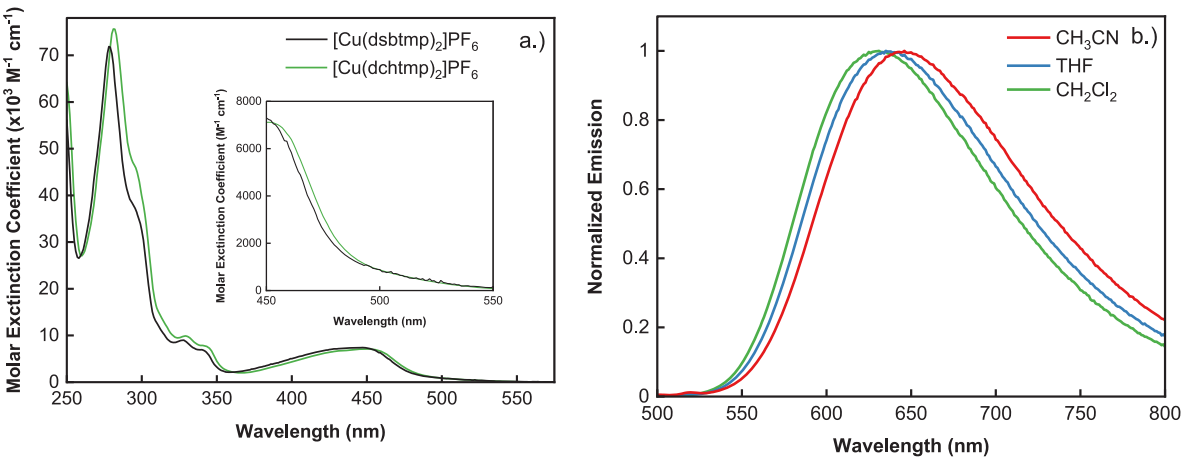

Figure 3. (a) Ground-state absorption spectrum of $[Cu(dchtmp)_2]PF_6$ (green) and $[Cu(dchtmp)_2]PF_6$[48] (black) measured in CH_2Cl_2. Inset figure of the low-intensity tail of the MLCT band. (b) Normalized PL spectra of $[Cu(dchtmp)_2]PF_6$ measured in deaerated CH_2Cl_2 (green), THF (blue), and CH_3CN (red)(λ_{ex} = 450 nm).

Table 2. Comparison of the Photophysical Properties of $[Cu(dchtmp)_2]PF_6$ and $[Cu(dsbtmp)_2]PF_6$[a]

solvent	λ_{Em} (nm)	Φ_{Em}[b] (%)	τ_{PL} (μs)	k_r ($\times 10^4$ s^{-1})	k_{nr} ($\times 10^5$ s^{-1})
			$[Cu(dchtmp)_2]PF_6$		
CH_2Cl_2	631	5.5 ± 0.4	2.6 ± 0.1	2.1 ± 0.2	3.6 ± 0.3
THF	639	3.7 ± 0.3	2.0 ± 0.1	1.9 ± 0.2	4.9 ± 0.5
CH_3CN	650	2.6 ± 0.3	1.5 ± 0.1	1.7 ± 0.2	6.5 ± 0.9
			$[Cu(dsbtmp)_2]PF_6$[c]		
CH_2Cl_2	631	6.3 ± 0.4	2.8	2.3	3.4
THF	639	5.3 ± 0.4[d]	2.1 ± 0.1	2.5 ± 0.2[d]	4.5 ± 0.4[d]
CH_3CN	649	2.9 ± 0.3	1.5	2.0	6.7

[a]Measured in deaerated solutions. [b]Absolute quantum yields. [c]From ref 48. [d]Newly reported values.

Variable Temperature Photoluminescence. The lowest energy ^{1}MLCT state of Cu(I) diimines lies closely in energy to the ^{3}MLCT state, enabling thermally activated delayed fluorescence (TADF) to be observed in these molecules at room temperature.[48,70−74] To determine the singlet−triplet energy gap in $[Cu(dchtmp)_2]PF_6$, the change in PL emission decay rate was measured at temperatures ranging between −100 and 60 °C in THF. As the temperature decreases, the repopulation of the ^{1}MLCT state becomes less favorable, yielding a longer PL emission decay lifetime. The relationship between the observed PL emission decay rates (k_{obs}) and temperature (T) can be modeled using eq 2,[72] where k_t and k_s are the triplet and singlet PL emission decay rates, respectively, ΔE is the energy gap of the singlet−triplet MLCT states, and k_b is the Boltzmann constant.

$$k_{obs} = \frac{3k_t + k_s \exp\left(-\frac{\Delta E}{k_b T}\right)}{3 + \exp\left(-\frac{\Delta E}{k_b T}\right)} \quad (2)$$

Using this treatment, a singlet−triplet energy gap of 1190 ± 90 cm^{-1} was found for $[Cu(dchtmp)_2]^+$ (Figures S19 and S20), consistent with that measured in previously investigated homoleptic Cu(I) *bis*(diimines).[14,48−50,71,73]

Nanosecond Transient Absorption Spectroscopy. The transient absorption difference spectra of $[Cu(dchtmp)_2]PF_6$ measured in deaerated CH_2Cl_2 following 450 nm laser pulses (1.6 mJ/pulse, 5−7 ns fwhm) taken across various time delays is presented in Figure 4. The MLCT ground state bleach is centered at 450 nm, but the difference spectrum is dominated by a blue excited state absorption at 350 nm and an intense double-top feature located at 530 and 570 nm resembling the electronic spectrum of the phenanthroline radical anion.[75] Both spectroscopic signatures are visualized throughout the transient absorption difference spectra of numerous related *bis*(homoleptic) Cu(I) phenanthrolines.[20,22,40,48,64] Transient absorption kinetics were adequately modeled using single exponential decays with lifetimes matching those measured using photoluminescence intensity decay data (Figure S21 and Table 2).

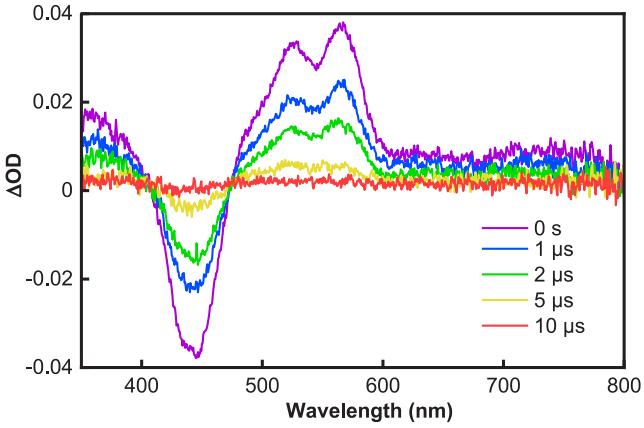

Figure 4. Transient absorption difference spectra of $[Cu(dchtmp)_2]PF_6$ in deaerated CH_2Cl_2 following 450 nm pulsed laser excitation (1.6 mJ/pulse, 5−7 fwhm) measured as a function of delay time.

https://doi.org/10.1021/acs.inorgchem.1c01242
Inorg. Chem. XXXX, XXX, XXX−XXX

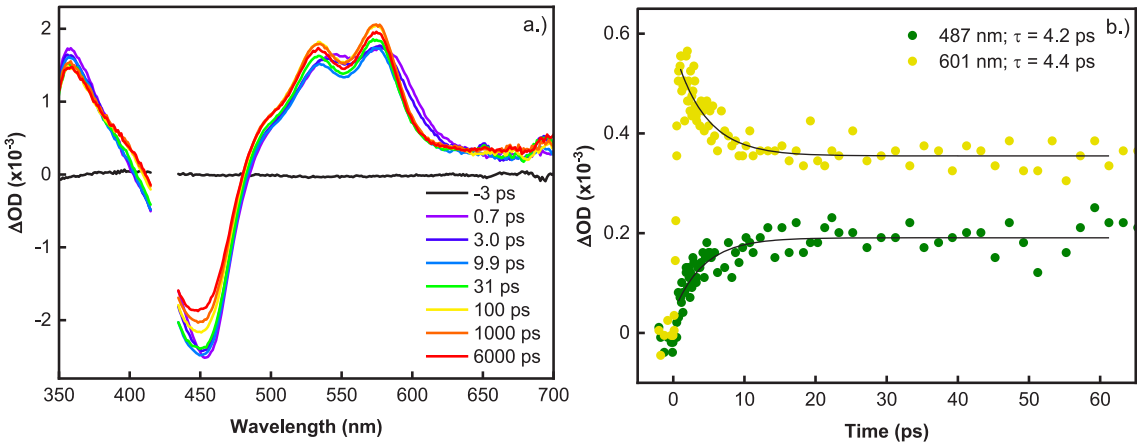

Figure 5. (a) Ultrafast transient absorption difference spectrum of $[Cu(dchtmp)_2]PF_6$ in CH_2Cl_2 excited by 425 nm pump beam (1.0 μJ/pulse). (b) Kinetic data of Figure 5a fit to a single exponential growth at 487 nm (τ = 4.2 ps) and a single exponential decay at 601 nm (τ = 4.4 ps).

Ultrafast Transient Absorption Spectroscopy. The ultrafast excited-state absorption difference spectra of $[Cu(dchtmp)_2]PF_6$ measured in CH_2Cl_2 following 425 nm excitation (1.0 μJ/pulse, 100 fs fwhm) are presented in Figure 5a. The difference spectra exhibit a ground-state MLCT bleach centered at 450 nm sandwiched between two positive excited state features. The UV transient absorption feature has a peak maximum at 360 nm, and the visible feature exhibits the same double-top profile from the nanosecond experiments that become more distinct after a 3.0 ps delay at 535 and 575 nm. These spectral signatures readily enable confident assignment of ^{3}MLCT formation.[40,49] These absorption features persist throughout the available experimental delay window of 6 ns, Figure 4, indicating that there is no further change in the excited-state species once the lowest ^{3}MLCT state is produced. Transient kinetic data taken from the red edge of the double-top feature and the ground-state bleach were used to assess the PJT distortion and ISC time constants. Single wavelength kinetic data recorded at 487 and 601 nm were fit to a single exponential decay and growth in Figure 5b, yielding time constants of 4.2 and 4.4 ps, respectively. These time constants are consistent with ISC from the singlet to triplet MLCT manifold of other sterically inhibited homoleptic Cu(I) diimine complexes.[40,41,49,63,70] Assignment of the PJT distortion was not possible here as single exponential functions adequately modeled the ultrafast data. As a result, we speculate that the PJT distortion may occur within the experimental IRF ~ 150 fs or that the molecule does not significantly distort due to the steric hindrance provided by the two cyclohexyl groups.[40]

■ CONCLUSIONS

A new homoleptic Cu(I) *bis*(phenanthroline) complex, $[Cu(dchtmp)_2]^+$, featuring 2,9-cycloalkyl substitutions was prepared and photophysically characterized. We have demonstrated that the photochemical ligand synthetic pathway successful for dchtmp could be extended to other cycloalkyl substituents exemplified in the dcptmp ligand. The failure of dcptmp to *bis*-coordinate to the Cu(I) center was rationalized in terms of the steric hindrance afforded by the half-chair conformer that ultimately preventing the coordination of a second ligand to form the desired homoleptic complex $[Cu(dcptmp)_2]^+$. This particular result gleans insight into the absolute limit of steric bulk possible afforded by the 2,9-cycloalkyl substituents on phenanthroline where preparation of the *bis*(homoleptic) Cu(I) species becomes improbable. $[Cu(dchtmp)_2]^+$ featured a 2.6 μs excited state lifetime in CH_2Cl_2 and maintains long lifetimes even in Lewis basic solvents such as CH_3CN where τ = 1.5 μs. The combined photophysical and electrochemical properties of the title complex essentially echo those of $[Cu(dsbtmp)_2]^+$.[48] Ultrafast transient absorption spectroscopy revealed a single time constant (τ = 4.4 ps) on ultrafast time regimes which was assigned to the intersystem crossing event from the ^{1}MLCT into the ^{3}MLCT state. The lack of a second experimentally resolvable ultrafast time constant suggests that either the PJT distortion occurred faster than our experimental IRF (<150 fs) or that the distortion was not significant enough to produce a unique optical signature for which a time constant could be assigned. Electrochemical studies in concert with static PL data enabled estimation of the excited state reduction potential of $[Cu(dchtmp)_2]^+$ (−1.77 V vs $Fc^{+/0}$ in CH_3CN), representative of a potent excited state reductant capable of driving photochemical synthesis and poised for solar photochemistry applications.

■ ASSOCIATED CONTENT

Supporting Information

The Supporting Information is available free of charge at https://pubs.acs.org/doi/10.1021/acs.inorgchem.1c01242.

Experimental methods, structural characterization data, additional static and time-resolved spectra, PL quenching experiments with DPA, temperature-dependent PL experiments, additional electronic structure calculation details, and the 3D structures (XYZ) of $[Cu(dmp)_2]^+$, $[Cu(hmp)_2]^+$, $[Cu(dsbtmp)_2]^+$, and $[Cu(dchtmp)_2]^+$ (PDF)

■ AUTHOR INFORMATION

Corresponding Author

Felix N. Castellano − *Department of Chemistry, North Carolina State University, Raleigh, North Carolina 27695-8204, United States;* orcid.org/0000-0001-7546-8618; Phone: (919) 515-3021; Email: fncastel@ncsu.edu

Authors

Michael C. Rosko − *Department of Chemistry, North Carolina State University, Raleigh, North Carolina 27695-8204, United States;* orcid.org/0000-0001-5392-8513

Kaylee A. Wells − *Department of Chemistry, North Carolina State University, Raleigh, North Carolina 27695-8204, United States;* orcid.org/0000-0002-6870-6574

Cory E. Hauke − *Department of Chemistry, North Carolina State University, Raleigh, North Carolina 27695-8204, United States;* orcid.org/0000-0001-8822-0961

Complete contact information is available at: https://pubs.acs.org/10.1021/acs.inorgchem.1c01242

Author Contributions

The manuscript was written through contributions of all authors. All authors have given approval to the final version of the manuscript.

Notes

The authors declare no competing financial interest.

■ ACKNOWLEDGMENTS

This work was supported by the U.S. Department of Energy, Office of Science, Office of Basic Energy Sciences, under Award Number DE-SC0011979. K.A.W. was supported by the National Science Foundation (CHE-1955795). We thank Dr. Frank Glorius at the University of Münster as well as Remi Fayed and Daniel T. Yonemoto at North Carolina State University for fruitful discussions.

■ REFERENCES

(1) Baranoff, E.; Collin, J.-P.; Flamigni, L.; Sauvage, J.-P. From Ruthenium(II) to Iridium(III): 15 Years of Triads Based on Bis-Terpyridine Complexes. *Chem. Soc. Rev.* **2004**, *33* (3), 147−155.

(2) Koike, T.; Akita, M. Visible-Light Radical Reaction Designed by Ru- and Ir-Based Photoredox Catalysis. *Inorg. Chem. Front.* **2014**, *1* (8), 562−576.

(3) Tóth, B. L.; Tischler, O.; Novák, Z. Recent Advances in Dual Transition Metal−Visible Light Photoredox Catalysis. *Tetrahedron Lett.* **2016**, *57* (41), 4505−4513.

(4) Tao, C.; Wang, B.; Sun, L.; Liu, Z.; Zhai, Y.; Zhang, X.; Wang, J. Merging Visible-Light Photoredox and Copper Catalysis in Catalytic Aerobic Oxidation of Amines to Nitriles. *Org. Biomol. Chem.* **2017**, *15* (2), 328−332.

(5) Wagenknecht, P. S.; Ford, P. C. Metal Centered Ligand Field Excited States: Their Roles in the Design and Performance of Transition Metal Based Photochemical Molecular Devices. *Coord. Chem. Rev.* **2011**, *255* (5), 591−616.

(6) Nia, N. Y.; Farahani, P.; Sabzyan, H.; Zendehdel, M.; Oftadeh, M. A Combined Computational and Experimental Study of the $[Co(bpy)_3]^{2+/3+}$ Complexes as One-Electron Outer-Sphere Redox Couples in Dye-Sensitized Solar Cell Electrolyte Media. *Phys. Chem. Chem. Phys.* **2014**, *16* (23), 11481−11491.

(7) Auböck, G.; Chergui, M. Sub-50-Fs Photoinduced Spin Crossover in [Fe(Bpy) 3] 2+. *Nat. Chem.* **2015**, *7* (8), 629−633.

(8) Larsen, C. B.; Wenger, O. S. Photoredox Catalysis with Metal Complexes Made from Earth-Abundant Elements. *Chem. - Eur. J.* **2018**, *24* (9), 2039−2058.

(9) Wenger, O. S. Photoactive Complexes with Earth-Abundant Metals. *J. Am. Chem. Soc.* **2018**, *140* (42), 13522−13533.

(10) Wehry, E. L.; Sundararajan, S. Intersystem Crossing and Internal Conversion from the Lowest Charge-Transfer Singlet Excited State of the (2,9-Dimethyl-1,10-Phenanthroline)Copper(I) Cation. *J. Chem. Soc., Chem. Commun.* **1972**, *20*, 1135−1136.

(11) Buckner, M. T.; McMillin, D. R. Photoluminescence from Copper(I) Complexes with Low-Lying Metal-to-Ligand Charge Transfer Excited States. *J. Chem. Soc., Chem. Commun.* **1978**, *17*, 759−761.

(12) Ahn, B.-T.; McMillin, D. R. Studies of Photoinduced Electron Transfer from Bis(2,9-Dimethyl-1,10-Phenanthroline)Copper(I). *Inorg. Chem.* **1978**, *17* (8), 2253−2258.

(13) Blaskie, M. W.; McMillin, D. R. Photostudies of Copper(I) Systems. 6. Room-Temperature Emission and Quenching Studies of Bis(2,9-Dimethyl-1,10-Phenanthroline)Copper(I). *Inorg. Chem.* **1980**, *19* (11), 3519−3522.

(14) Kirchhoff, J. R.; Gamache, R. E.; Blaskie, M. W.; Del Paggio, A. A.; Lengel, R. K.; McMillin, D. R. Temperature Dependence of Luminescence from $Cu(NN)^{2+}$ Systems in Fluid Solution. Evidence for the Participation of Two Excited States. *Inorg. Chem.* **1983**, *22* (17), 2380−2384.

(15) Phifer, C. C.; McMillin, D. R. The Basis of Aryl Substituent Effects on Charge-Transfer Absorption Intensities. *Inorg. Chem.* **1986**, *25* (9), 1329−1333.

(16) McGarvey, J. J.; Bell, S. E. J.; Gordon, K. C. Single- and Two-Color Pulsed Laser Resonance Raman Spectroscopy of Excited States of Bis(2,9-Dimethyl-1,10-Phenanthroline)Copper(I) in Solution. *Inorg. Chem.* **1988**, *27* (22), 4003−4006.

(17) Crane, D. R.; Ford, P. C. Activation Volume ($\Delta V^{\ddagger}q$) for Energy- and Electron-Transfer Quenching of [Cu(dpp)2+]* (dpp = 2,9-Diphenyl-1,10-Phenanthroline). *Inorg. Chem.* **1993**, *32* (11), 2391−2393.

(18) Chi-Ying, H.; Tie-Lin, W.; Zhiqiang, S.; Thummel, R. P. A Friedländer Approach to Novel 1,10-Phenanthrolines and Their Use as Ligands for Ru(II) and Cu(I). *Tetrahedron* **1994**, *50* (36), 10685−10692.

(19) Pallenberg, A. J.; Koenig, K. S.; Barnhart, D. M. Synthesis and Characterization of Some Copper(I) Phenanthroline Complexes. *Inorg. Chem.* **1995**, *34* (11), 2833−2840.

(20) Armaroli, N.; Rodgers, M. A. J.; Ceroni, P.; Balzani, V.; Dietrich-Buchecker, C. O.; Kern, J.-M.; Bailal, A.; Sauvage, J.-P. Nature of the Lowest Energy Excited State of a Bis-Phenanthroline [2]-Catenane and Its Cu(I), Ag(I) and Co(II) Complexes. *Chem. Phys. Lett.* **1995**, *241* (5), 555−558.

(21) Eggleston, M. K.; Fanwick, P. E.; Pallenberg, A. J.; McMillin, D. R. A Twist on the Copper Center in the Crystal Structure of $[Cu(dnpp)_2]PF_6$ and the Charge-Transfer Excited State? (dnpp = 2,9-Dineopentyl-1,10-Phenanthroline). *Inorg. Chem.* **1997**, *36* (18), 4007−4010.

(22) Chen, L. X.; Jennings, G.; Liu, T.; Gosztola, D. J.; Hessler, J. P.; Scaltrito, D. V.; Meyer, G. J. Rapid Excited-State Structural Reorganization Captured by Pulsed X-Rays. *J. Am. Chem. Soc.* **2002**, *124* (36), 10861−10867.

(23) Chen, L. X.; Shaw, G. B.; Novozhilova, I.; Liu, T.; Jennings, G.; Attenkofer, K.; Meyer, G. J.; Coppens, P. MLCT State Structure and Dynamics of a Copper(I) Diimine Complex Characterized by Pump−Probe X-Ray and Laser Spectroscopies and DFT Calculations. *J. Am. Chem. Soc.* **2003**, *125* (23), 7022−7034.

(24) Leydet, Y.; Bassani, D. M.; Jonusauskas, G.; McClenaghan, N. D. Equilibration between Three Different Excited States in a Bichromophoric Copper(I) Polypyridine Complex. *J. Am. Chem. Soc.* **2007**, *129* (28), 8688−8689.

(25) Gandhi, B. A.; Green, O.; Burstyn, J. N. Facile Oxidation-Based Synthesis of Sterically Encumbered Four-Coordinate Bis(2,9-Di- *Tert* -Butyl-1,10-Phenanthroline)Copper(I) and Related Three-Coordinate Copper(I) Complexes. *Inorg. Chem.* **2007**, *46* (10), 3816−3825.

(26) Laviecambot, A.; Cantuel, M.; Leydet, Y.; Jonusauskas, G.; Bassani, D.; Mcclenaghan, N. Improving the Photophysical Properties of Copper(I) Bis(Phenanthroline) Complexes. *Coord. Chem. Rev.* **2008**, *252* (23−24), 2572−2584.

(27) Gothard, N. A.; Mara, M. W.; Huang, J.; Szarko, J. M.; Rolczynski, B.; Lockard, J. V.; Chen, L. X. Strong Steric Hindrance Effect on Excited State Structural Dynamics of Cu(I) Diimine Complexes. *J. Phys. Chem. A* **2012**, *116* (9), 1984−1992.

(28) Lazorski, M. S.; Castellano, F. N. Advances in the Light Conversion Properties of Cu(I)-Based Photosensitizers. *Polyhedron* **2014**, *82*, 57−70.

(29) Soulis, K.; Gourlaouen, C.; Daniel, C.; Quatela, A.; Odobel, F.; Blart, E.; Pellegrin, Y. New Luminescent Copper(I) Complexes with Extended π-Conjugation. *Polyhedron* **2018**, *140*, 42−50.

(30) Brown-Xu, S.; Fumanal, M.; Gourlaouen, C.; Gimeno, L.; Quatela, A.; Thobie-Gautier, C.; Blart, E.; Planchat, A.; Riobé, F.; Monnereau, C.; Chen, L. X.; Daniel, C.; Pellegrin, Y. Intriguing Effects of Halogen Substitution on the Photophysical Properties of 2,9-(Bis)Halo-Substituted Phenanthrolinecopper(I) Complexes. *Inorg. Chem.* **2019**, *58* (12), 7730−7745.

(31) Livshits, M. Y.; Reeves, B. J.; DeWeerd, N. J.; Strauss, S. H.; Boltalina, O. V.; Rack, J. J. Trifluoromethylated Phenanthroline Ligands Reduce Excited-State Distortion in Homoleptic Copper(I) Complexes. *Inorg. Chem.* **2020**, *59* (5), 2781−2790.

(32) Bersuker, I. B. Pseudo-Jahn−Teller Effect—A Two-State Paradigm in Formation, Deformation, and Transformation of Molecular Systems and Solids. *Chem. Rev.* **2013**, *113* (3), 1351−1390.

(33) Riesgo, E. C.; Hu, Y.-Z.; Bouvier, F.; Thummel, R. P.; Scaltrito, D. V.; Meyer, G. J. Crowded Cu(I) Complexes Involving Benzo[h]-Quinoline: π-Stacking Effects and Long-Lived Excited States. *Inorg. Chem.* **2001**, *40* (14), 3413−3422.

(34) Dietrich-Buchecker, C. O.; Marnot, P. A.; Sauvage, J.-P.; Kirchhoff, J. R.; McMillin, D. R. Bis(2,9-Diphenyl-1,10-Phenanthroline)Copper(I): A Copper Complex with a Long-Lived Charge-Transfer Excited State. *J. Chem. Soc., Chem. Commun.* **1983**, *9*, 513−515.

(35) McMillin, D. R.; Kirchhoff, J. R.; Goodwin, K. V. Exciplex Quenching of Photo-Excitd Copper Complexes. *Coord. Chem. Rev.* **1985**, *64*, 83−92.

(36) Palmer, C. E. A.; McMillin, D. R.; Kirmaier, C.; Holten, D. Flash Photolysis and Quenching Studies of Copper(I) Systems in the Presence of Lewis Bases: Inorganic Exciplexes? *Inorg. Chem.* **1987**, *26* (19), 3167−3170.

(37) Everly, R. M.; McMillin, D. R. Concentration-Dependent Lifetimes of $Cu(NN)^{+2}$ Systems: Exciplex Quenching from the Ion Pair State. *Photochem. Photobiol.* **1989**, *50* (6), 711−716.

(38) Shaw, G. B.; Grant, C. D.; Shirota, H.; Castner, E. W.; Meyer, G. J.; Chen, L. X. Ultrafast Structural Rearrangements in the MLCT Excited State for Copper(I) Bis-Phenanthrolines in Solution. *J. Am. Chem. Soc.* **2007**, *129* (7), 2147−2160.

(39) Mara, M. W.; Fransted, K. A.; Chen, L. X. Interplays of Excited State Structures and Dynamics in Copper(I) Diimine Complexes: Implications and Perspectives. *Coord. Chem. Rev.* **2015**, *282*−*283*, 2−18.

(40) Garakyaraghi, S.; Danilov, E. O.; McCusker, C. E.; Castellano, F. N. Transient Absorption Dynamics of Sterically Congested Cu(I) MLCT Excited States. *J. Phys. Chem. A* **2015**, *119* (13), 3181−3193.

(41) Iwamura, M.; Takeuchi, S.; Tahara, T. Ultrafast Excited-State Dynamics of Copper(I) Complexes. *Acc. Chem. Res.* **2015**, *48* (3), 782−791.

(42) Siddique, Z. A.; Yamamoto, Y.; Ohno, T.; Nozaki, K. Structure-Dependent Photophysical Properties of Singlet and Triplet Metal-to-Ligand Charge Transfer States in Copper(I) Bis(Diimine) Compounds. *Inorg. Chem.* **2003**, *42* (20), 6366−6378.

(43) Iwamura, M.; Takeuchi, S.; Tahara, T. Substituent Effect on the Photoinduced Structural Change of Cu(I) Complexes Observed by Femtosecond Emission Spectroscopy. *Phys. Chem. Chem. Phys.* **2014**, *16* (9), 4143−4154.

(44) Green, O.; Gandhi, B. A.; Burstyn, J. N. Photophysical Characteristics and Reactivity of Bis(2,9-Di-Tert-Butyl-1,10-Phenanthroline)Copper(I). *Inorg. Chem.* **2009**, *48* (13), 5704−5714.

(45) Eggleston, M. K.; McMillin, D. R.; Koenig, K. S.; Pallenberg, A. J. Steric Effects in the Ground and Excited States of $Cu(NN)^{2+}$ Systems. *Inorg. Chem.* **1997**, *36* (2), 172−176.

(46) Appleton, J. L.; Silber, V.; Karmazin, L.; Bailly, C.; Chambron, J.-C.; Weiss, J.; Ruppert, R. A New Phenanthroline Ligand and the Spontaneous Resolution of Its Homoleptic Copper(I) Complex. *Eur. J. Org. Chem.* **2020**, *2020* (47), 7320−7326.

(47) Cunningham, C. T.; Cunningham, K. L. H.; Michalec, J. F.; McMillin, D. R. Cooperative Substituent Effects on the Excited States of Copper Phenanthrolines. *Inorg. Chem.* **1999**, *38* (20), 4388−4392.

(48) McCusker, C. E.; Castellano, F. N. Design of a Long-Lifetime, Earth-Abundant, Aqueous Compatible Cu(I) Photosensitizer Using Cooperative Steric Effects. *Inorg. Chem.* **2013**, *52* (14), 8114−8120.

(49) Garakyaraghi, S.; Crapps, P. D.; McCusker, C. E.; Castellano, F. N. Cuprous Phenanthroline MLCT Chromophore Featuring Synthetically Tailored Photophysics. *Inorg. Chem.* **2016**, *55* (20), 10628−10636.

(50) Garakyaraghi, S.; McCusker, C. E.; Khan, S.; Koutnik, P.; Bui, A. T.; Castellano, F. N. Enhancing the Visible-Light Absorption and Excited-State Properties of Cu(I) MLCT Excited States. *Inorg. Chem.* **2018**, *57* (4), 2296−2307.

(51) Dietrick-Buchecker, C. O.; Marnot, P. A.; Sauvage, J. P. Direct Synthesis of Disubstituted Aromatic Polyimine Chelates. *Tetrahedron Lett.* **1982**, *23* (50), 5291−5294.

(52) Klauck, F. J. R.; James, M. J.; Glorius, F. Deaminative Strategy for the Visible-Light-Mediated Generation of Alkyl Radicals. *Angew. Chem., Int. Ed.* **2017**, *56* (40), 12336−12339.

(53) Monos, T. M.; Sun, A. C.; McAtee, R. C.; Devery, J. J.; Stephenson, C. R. J. Microwave-Assisted Synthesis of Heteroleptic $Ir(III)^{+}$ Polypyridyl Complexes. *J. Org. Chem.* **2016**, *81* (16), 6988−6994.

(54) Kubas, G. J.; Monzyk, B.; Crumbliss, A. L. Tetrakis-(Acetonitrile)Copper(I) Hexafluorophosphate. In *Inorganic Syntheses*; John Wiley & Sons, Ltd, 1979; 90−92. DOI: 10.1002/9780470132500.ch18.

(55) Frisch, M. J.; Trucks, G. W.; Schlegel, H. B.; Scuseria, G. E.; Robb, M. A.; Cheeseman, J. R.; Scalmani, G.; Petersson, G. A.; et al. *Gaussian 16*, Rev. A.03; Gaussian Inc: Wallingford, CT, 2016.

(56) Hehre, W. J.; Ditchfield, R.; Pople, J. A. Self—Consistent Molecular Orbital Methods. XII. Further Extensions of Gaussian—Type Basis Sets for Use in Molecular Orbital Studies of Organic Molecules. *J. Chem. Phys.* **1972**, *56*, 2257−2261.

(57) Lee, C.; Yang, W.; Parr, R. G. Development of the Colle-Salvetti Correlation-Energy Formula into a Functional of the Electron Density. *Phys. Rev. B: Condens. Matter Mater. Phys.* **1988**, *37* (2), 785−789.

(58) Becke, A. D. Density-functional Thermochemistry. III. The Role of Exact Exchange. *J. Chem. Phys.* **1993**, *98* (7), 5648−5652.

(59) Grimme, S.; Antony, J.; Ehrlich, S.; Krieg, H. A Consistent and Accurate Ab Initio Parametrization of Density Functional Dispersion Correction (DFT-D) for the 94 Elements H-Pu. *J. Chem. Phys.* **2010**, *132* (15), 154104.

(60) Dolg, M.; Wedig, U.; Stoll, H.; Preuss, H. Energy-adjusted Ab Initio Pseudopotentials for the First Row Transition Elements. *J. Chem. Phys.* **1987**, *86* (2), 866−872.

(61) Cossi, M.; Scalmani, G.; Rega, N.; Barone, V. New Developments in the Polarizable Continuum Model for Quantum Mechanical and Classical Calculations on Molecules in Solution. *J. Chem. Phys.* **2002**, *117* (1), 43−54.

(62) Dennington, R.; Kieth, T. A.; Milliam, J. M. *Gauss View*, Version 6; Semichem Inc.: Shawnee Mission, KS, 2016.

(63) Garakyaraghi, S.; Koutnik, P.; Castellano, F. N. Photoinduced Structural Distortions and Singlet−Triplet Intersystem Crossing in Cu(I) MLCT Excited States Monitored by Optically Gated Fluorescence Spectroscopy. *Phys. Chem. Chem. Phys.* **2017**, *19* (25), 16662−16668.

(64) Ruthkosky, M.; Castellano, F. N.; Meyer, G. J. Photodriven Electron and Energy Transfer from Copper Phenanthroline Excited States. *Inorg. Chem.* **1996**, *35* (22), 6406−6412.

(65) Bock, C. R.; Connor, J. A.; Gutierrez, A. R.; Meyer, T. J.; Whitten, D. G.; Sullivan, B. P.; Nagle, J. K. Estimation of Excited-State Redox Potentials by Electron-Transfer Quenching. Application of Electron-Transfer Theory to Excited-State Redox Processes. *J. Am. Chem. Soc.* **1979**, *101* (17), 4815−4824.

https://doi.org/10.1021/acs.inorgchem.1c01242
Inorg. Chem. XXXX, XXX, XXX−XXX

(66) Hockin, B. M.; Li, C.; Robertson, N.; Zysman-Colman, E. Photoredox Catalysts Based on Earth-Abundant Metal Complexes. *Catal. Sci. Technol.* **2019**, *9* (4), 889−915.

(67) Armaroli, N.; De Cola, L.; Balzani, V.; Sauvage, J.-P.; Dietrich-Buchecker, C. O.; Kern, J.-M. Absorption and Luminescence Properties of 1,10-Phenanthroline, 2,9-Diphenyl-1,10-Phenanthroline, 2,9-Dianisyl-1,10-Phenanthroline and Their Protonated Forms in Dichloromethane Solution. *J. Chem. Soc., Faraday Trans.* **1992**, *88*, 553.

(68) Scaltrito, D. V.; Thompson, D. W.; O'Callaghan, J. A.; Meyer, G. J. MLCT Excited States of Cuprous Bis-Phenanthroline Coordination Compounds. *Coord. Chem. Rev.* **2000**, *208* (1), 243−266.

(69) Parker, W. L.; Crosby, G. A. Assignment of the Charge-Transfer Excited States of Bis(N-Heterocyclic) Complexes of Copper(I). *J. Phys. Chem.* **1989**, *93* (15), 5692−5696.

(70) Iwamura, M.; Takeuchi, S.; Tahara, T. Real-Time Observation of the Photoinduced Structural Change of Bis(2,9-Dimethyl-1,10-Phenanthroline)Copper(I) by Femtosecond Fluorescence Spectroscopy: A Realistic Potential Curve of the Jahn−Teller Distortion. *J. Am. Chem. Soc.* **2007**, *129* (16), 5248−5256.

(71) Asano, M. S.; Tomiduka, K.; Sekizawa, K.; Yamashita, K.; Sugiura, K. Temperature-Dependent Emission of Copper(I) Phenanthroline Complexes with Bulky Substituents: Estimation of an Energy Gap between the Singlet and Triplet MLCT States. *Chem. Lett.* **2010**, *39* (4), 376−378.

(72) Deaton, J. C.; Switalski, S. C.; Kondakov, D. Y.; Young, R. H.; Pawlik, T. D.; Giesen, D. J.; Harkins, S. B.; Miller, A. J. M.; Mickenberg, S. F.; Peters, J. C. E-Type Delayed Fluorescence of a Phosphine-Supported $Cu_2(\mu\text{-}NAr_2)_2$ Diamond Core: Harvesting Singlet and Triplet Excitons in OLEDs. *J. Am. Chem. Soc.* **2010**, *132* (27), 9499−9508.

(73) Czerwieniec, R.; Yersin, H. Diversity of Copper(I) Complexes Showing Thermally Activated Delayed Fluorescence: Basic Photophysical Analysis. *Inorg. Chem.* **2015**, *54* (9), 4322−4327.

(74) Lv, L.; Yuan, K.; Wang, Y. Theoretical Studying of Basic Photophysical Processes in a Thermally Activated Delayed Fluorescence Copper(I) Complex: Determination of Reverse Intersystem Crossing and Radiative Rate Constants. *Org. Electron.* **2017**, *51*, 207−219.

(75) Kato, T.; Shida, T. Electronic Structures of Ion Radicals of Nitrogen-Heteroaromatic Hydrocarbons as Studied by ESR and Optical Spectroscopy. *J. Am. Chem. Soc.* **1979**, *101* (23), 6869−6876.

https://doi.org/10.1021/acs.inorgchem.1c01242
Inorg. Chem. XXXX, XXX, XXX−XXX